



Alkalinization Scenarios in the Mediterranean Sea for Efficient Removal of Atmospheric CO₂ and the Mitigation of Ocean Acidification

Momme Butenschön^{1*}, Tomas Lovato¹, Simona Masina¹, Stefano Caserini² and Mario Grosso²

¹ Ocean Modeling and Data Assimilation Division, Centro Euro-Mediterraneo sui Cambiamenti Climatici, Bologna, Italy,

² Dipartimento di Ingegneria Civile e Ambientale, Politecnico di Milano, Milan, Italy

OPEN ACCESS

Edited by:

David Peter Keller,
GEOMAR Helmholtz Center for Ocean
Research Kiel, Germany

Reviewed by:

Peter Köhler,
Alfred Wegener Institute Helmholtz
Center for Polar and Marine Research,
Germany
Friederike Fröb,
Max Planck Society, Germany

*Correspondence:

Momme Butenschön
momme.butenschon@cmcc.it

Specialty section:

This article was submitted to
Negative Emission Technologies,
a section of the journal
Frontiers in Climate

Received: 06 October 2020

Accepted: 12 February 2021

Published: 18 March 2021

Citation:

Butenschön M, Lovato T, Masina S,
Caserini S and Grosso M (2021)
Alkalinization Scenarios in the
Mediterranean Sea for Efficient
Removal of Atmospheric CO₂ and the
Mitigation of Ocean Acidification.
Front. Clim. 3:614537.
doi: 10.3389/fclim.2021.614537

It is now widely recognized that in order to reach the target of limiting global warming to well below 2°C above pre-industrial levels (as the objective of the Paris agreement), cutting the carbon emissions even at an unprecedented pace will not be sufficient, but there is the need for development and implementation of active Carbon Dioxide Removal (CDR) strategies. Among the CDR strategies that currently exist, relatively few studies have assessed the mitigation capacity of ocean-based Negative Emission Technologies (NET) and the feasibility of their implementation on a larger scale to support efficient implementation strategies of CDR. This study investigates the case of ocean alkalinization, which has the additional potential of contrasting the ongoing acidification resulting from increased uptake of atmospheric CO₂ by the seas. More specifically, we present an analysis of marine alkalinization applied to the Mediterranean Sea taking into consideration the regional characteristics of the basin. Rather than using idealized spatially homogenous scenarios of alkalinization as done in previous studies, which are practically hard to implement, we use a set of numerical simulations of alkalinization based on current shipping routes to quantitatively assess the alkalinization efficiency via a coupled physical-biogeochemical model (NEMO-BFM) for the Mediterranean Sea at 1/16° horizontal resolution (~6 km) under an RCP4.5 scenario over the next decades. Simulations suggest the potential of nearly doubling the carbon-dioxide uptake rate of the Mediterranean Sea after 30 years of alkalinization, and of neutralizing the mean surface acidification trend of the baseline scenario without alkalinization over the same time span. These levels are achieved via two different alkalinization strategies that are technically feasible using the current network of cargo and tanker ships: a first approach applying annual discharge of 200 Mt Ca(OH)₂ constant over the alkalinization period and a second approach with gradually increasing discharge proportional to the surface pH trend of the baseline scenario, reaching similar amounts of annual discharge by the end of the alkalinization period. We demonstrate that the latter approach allows to stabilize the mean surface pH at present day values and substantially increase the potential to counteract acidification relative to the alkalinity added, while the carbon uptake efficiency (mole of CO₂ absorbed by the ocean per mole of alkalinity added) is only marginally

reduced. Nevertheless, significant local alterations of the surface pH persist, calling for an investigation of the physiological and ecological implications of the extent of these alterations to the carbonate system in the short to medium term in order to support a safe, sustainable application of this CDR implementation.

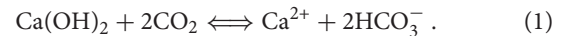
Keywords: climate change mitigation, ocean acidification, ocean alkalinization, Mediterranean sea, carbon dioxide removal, negative emission technologies, regional ocean model

1. INTRODUCTION

The Paris agreement of 2015 has set a cornerstone in international climate policy by defining the goal of limiting global warming to well below 2°C, a goal that is driven by the necessity to avoid irreversible change and to restrain intolerable risks to humanity, and supported by the feasibility to achieve this goal and by its simplicity as a tangible target bridging the communication gap between science and policy (Schellnhuber et al., 2016). It is widely accepted that to achieve this goal, it will not be sufficient to limit CO₂ emissions, but it will require the implementation of active CO₂ removal from the atmosphere (CDR) via negative emission technologies (NETs) (IPCC, 2018), as confirmed by the most recent generation of climate model projections within the CMIP6 initiative (Tokarska et al., 2020). Several candidates of NETs have been discussed in the past. Williamson (2016) has underlined that the requirement of the implementation of NETs to reach the goals of the Paris agreement calls for a broad assessment of the viability of CDR and demands urgent action. While some studies have emerged that assess NETs in theoretical, idealized experiments (e.g., Keller et al., 2014), high-level reports of various international bodies have identified the gap in current knowledge between these scientific intellectual exercises investigating the potential of a given NET and the feasibility of their practical implementation (Renforth and Wilcox, 2020). The ocean plays a particular role in the climate system acting as significant sink of atmospheric heat and CO₂ due to its greater heat capacity, solubility, and inertia. Recent estimates suggest that the ocean has taken up more than 90% of the excess heat in the climate system since 1970 and 20–30% of anthropogenic carbon since the 1980s (IPCC, 2019; von Schuckmann et al., 2020). This has caused the additional hazard of ocean acidification lowering the average pH of the ocean surface by approximately 0.017–0.027 units per decade. The pH alteration of ocean seawater since the pre-industrial period, that is unprecedented in the last 65 million years (Hoegh-Guldberg et al., 2018), has significant implications for marine organisms affecting their metabolic regulation and capability to form calcium carbonate (Kroeker et al., 2013), destabilizing the ecosystem and ultimately threatening vital ecosystem services (Gattuso et al., 2015).

Among the ocean-based NETs, artificial ocean alkalinization via the dissolution of Ca(OH)₂, known in short as ocean liming, has attracted attention due to its capability of contemporarily addressing two issues: global warming via increased uptake of CO₂ and ocean acidification. The principle behind ocean liming is based on the dissociation

of calcium hydroxide and carbon-dioxide to calcium ions and bicarbonate:



Hence, per mole of added slaked lime this reaction in principle consumes two moles of aqueous CO₂ increasing the alkalinity of the water body by two mole equivalents. It should be noted however, that this consumption of aqueous CO₂ does not correspond directly to a removal of atmospheric CO₂, which instead depends on the difference in partial pressure of CO₂ between sea and atmosphere at the water surface. The concentrations of dissolved inorganic carbon species within the carbonate system resulting from the reactions above adjust to a new equilibrium state depending on the environmental conditions in place (Zeebe and Wolf-Gladrow, 2001) and part of the added alkalinity is removed from the surface through advective, diffusive processes, and convection. The combination of these processes, along with the local temperature, salinity, and pressure, ultimately determine the partial pressure of CO₂ in the seawater and its pH. Furthermore, the production of slaked lime itself generates a considerable amount of CO₂ (Renforth et al., 2013). Even if the generated carbon-dioxide is generally of high purity and therefore feasible for geological storage, this underpins the requirement of CO₂ and cost-efficient technologies to provide slaked lime. In response to this challenge, Caserini et al. (2019) have proposed a combination of ocean liming, CO₂ storage and commercial industrial technologies producing H₂ as a by-product, that significantly improves the efficiency and reduces the cost of the overall process, but ultimately any full-scale implementation will need to be carefully balanced against the projected cost of CO₂ emissions.

Several studies have investigated the mitigation potential of ocean liming applications at the global scales via model projections of theoretical alkalinization scenarios following different strategies. Ilyina et al. (2013) used a global ocean biogeochemistry model to project a suite of scenarios with alkalinization levels applied homogeneously over areas of varying extent proportional to anthropogenic CO₂ emissions, corresponding to about 2.4 Pmol/y of alkalinity (approximately 89 Pg Ca(OH)₂/y) in the initial phase of the experiment, based on a scenario of rapid growth supported by intermediate use of fossil energy sources (SRES A1B). In their conclusions the authors indicate that a 2:1 molar ratio of added alkalinity per emitted CO₂ applied over a large area is required to fully counteract the decrease in mean global surface ocean pH, leading however to local conditions in the carbonate chemistry that exceed significantly from the range of natural variability. Keller

et al. (2014) projected in an Earth System Model a scenario of alkalinity discharge at $10 \text{ Pg Ca(OH)}_2/\text{y}$ uniform in space and time corresponding roughly to the maximum carrying capacity of large cargo and tanker ships against an RCP8.5 baseline scenario, finding that even at this scale the potential in terms of mitigating atmospheric CO_2 levels and consequently global warming are marginal. Lenton et al. (2018) implemented a similar scenario with a global annual discharge of 0.25 Pmol/y ($\sim 9.3 \text{ Pg Ca(OH)}_2/\text{y}$), but based on two opposing baselines of unmitigated (RCP8.5) vs. strongly mitigated (RCP2.6) climate change, revealing a significantly higher relative efficiency at lower emissions. In addition they showed a low sensitivity of the process when applied to large latitudinal bands or in different seasons with respect to a spatial and temporal homogeneous application of alkalization. González and Ilyina (2016) constructed an alkalization scenario based on a RCP8.5 with gradually increasing alkalinity additions calibrated to reach the atmospheric CO_2 levels of a corresponding RCP4.5 projection, concluding that 114 Pmol would be required to achieve the goal over the period from 2018 to 2100, at the price of unprecedented ocean biogeochemistry perturbations with unknown ecological consequences. None of these works however considered the practicalities of an actual large-scale implementation of ocean liming or investigated the relative efficiencies and sensitivities of different strategies with respect to the oceanic uptake of CO_2 and the mitigation of ocean acidification.

Here we propose a quantitative study of the potential of a practical, regional implementation of ocean liming to the Mediterranean Sea based on the existing network of tankers and cargo ships. The regional application of ocean liming to the Mediterranean Sea is supported by two factors: its wide coverage through existing shipping routes across the basin and its physical and biogeochemical characteristics. In fact, its strategic location enclosed by three continents and providing a short-cut connecting two ocean basins via the Suez channel results in a dense network of shipping traffic (see section 2). Such commercial routes provide an opportunity for the implementation of ocean liming using existing traffic as vehicle to distribute lime across the basin with very limited additional cost due to increased load ballast.

At the same time the physical characteristics of the semi-enclosed basin with only a small opening at the Gibraltar Strait strongly dominated by surface inflow, and with strong major currents leading to wide circulation patterns with small overturning cells at the Northern parts of the two sub-basins (Millot and Taupier-Letage, 2005; Pinardi et al., 2019) lead to an efficient distribution of discharged lime across the area limiting uncontrolled dispersal into confining waters. Moreover, the region represents an area of accumulation of anthropogenic carbon uptake (IPCC, 2013; Khatiwala et al., 2013; Palmiéri et al., 2015) and is generally recognized as a hotspot of climate change (Giorgi, 2006; UNEP/MAP, 2017) showing clear trends of warming and acidification across virtually the entire basin (MedSea, 2014; Lacoue-Labarthe et al., 2016; Soto-Navarro et al., 2020), which are nevertheless subject to high regional variability depending on physical (stratification, overturning) and biogeochemical features (productivity, alkalinity).

Alkalinization in the Mediterranean Sea is assessed in this study following two different approaches of lime discharge: a constant annual discharge and a time-varying approach based on the acidification trend of the basin without alkalization. This strategy allows us to assess the evolution of the system for each individual approach and compare their respective potentials in mitigating the atmospheric CO_2 increases and the ocean acidification.

2. METHODS

The model simulations performed in this study are ocean-only experiments of a regional marine biogeochemical model system with concentration driven atmospheric boundary conditions of CO_2 . It should be noted that this approach does not include feedback processes of the marine carbonate chemistry with the atmospheric concentrations, which is nevertheless justifiable in this context as the increase of the carbon sink due to alkalization across the Mediterranean Sea emerging from this study is expected to be small compared to the global atmospheric carbon reservoir (approximately 800 GtC , Friedlingstein et al., 2019) and due to the swift adjustment of the atmospheric concentrations given the rapid mixing time scales of the atmospheric dynamics. It allows for simulations of multiple decades of different alkalization scenarios required for the purpose of this work at resolutions that resolve the Mediterranean Sea dynamics, which would be unfeasible in a fully coupled system.

2.1. NEMO-BFM Model

The model used to simulate the marine physical and biogeochemical dynamics is composed by the general circulation ocean model NEMO (v3.4, Madec et al., 2013) and the Biogeochemical Flux Model (BFM v5.2, Vichi et al., 2020). Its application to the Mediterranean Sea relies on a spatial grid with a horizontal resolution of $1/16^\circ$ degree (which corresponds to about 6.5 km) and a vertical z -coordinate discretization in 72 levels, with spacing ranging from 3 m in surface layer to 350 m at the bottom. The parameterizations and numerical schemes used to resolve the physical processes are thoroughly described in Oddo et al. (2009), therein referred to as MFS_V2.2 configuration. With respect to previous applications of the BFM (Lazzari et al., 2012; Cossarini et al., 2015; Visinelli et al., 2016), the ecosystem structure setup for the present work can be considered a light-weight implementation that accounts for two primary producers (Diatoms and Nanoflagellates) and two predator types (Micro- and Meso-zooplankton). A key difference is the representation of zooplankton and bacteria functional groups at fixed stoichiometric ratios. A total of 32 state variables are considered in the model, including dissolved inorganic constituents and dissolved and particulate organic matter. The parametrization of living and nonliving functional rates derives from Vichi et al. (2013). The carbonate system dynamics described by the prognostic evolution of Dissolved Inorganic Carbon (DIC) and Total Alkalinity (TA) and parameterizations for chemical dissociation rates and gas exchanges were set in agreement with the protocol described in Orr et al. (2017).

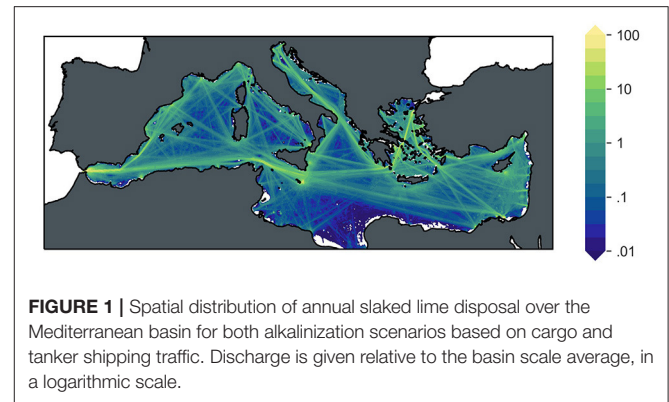
2.2. Reference Simulation

A reference experiment was designed to reproduce the physical and biogeochemical evolution of the Mediterranean Sea determined by the meteorological forcing representative of present and future conditions under the RCP4.5 scenario (Moss et al., 2010), namely for the 2000–2050 period. In contrast to most previous works on ocean alkalinization that are based on scenarios with comparatively high levels of greenhouse gas concentrations (RCP8.5 or SRES A1B) we chose a scenario with an intermediate concentration pathway as baseline to recognize the fact that liming on its own is unlikely sufficient as a mitigation measure against global warming (e.g., Ilyina et al., 2013; Keller et al., 2014) and unlikely to be applied as a single strategy, but in combination with other mitigation strategies. In fact, a strong commitment to greenhouse gas emission reductions has been declared within the UNFCCC process (UNFCCC, 2020) and net-zero emission targets have been declared by 823 cities, 101 regions, and 1541 companies (Data-Driven EnviroLab and NewClimate Institute, 2020).

Physical boundary conditions were extracted from the CMIP5 dataset of the atmosphere-ocean global circulation model CMCC-CM (Scoccimarro et al., 2011) and consist of 6-hourly atmospheric fields, daily fresh water discharges (rivers and Black Sea exchange), and monthly fields of temperature, salinity, and velocities prescribed at the open lateral boundaries in the neighboring parts of the Atlantic ocean (see Lovato et al., 2013 for technical details). The initial conditions for seawater temperature, salinity, dissolved oxygen, nitrate, phosphate, and silicate were derived from the SeaDataNet database (<http://www.seadatanet.org/>), while for DIC and TA two gridded datasets were blended in correspondence of the Gibraltar Strait: GLODAPv2 (Olsen et al., 2016) for the Atlantic region and the reconstructed fields of Lovato and Vichi (2015) for the Mediterranean sea. Biogeochemical properties at the lateral open boundaries were solved with a zero-gradient condition, as the Atlantic region included in the model is big enough to allow for internal adjustment of the ecosystem dynamics with minor drifts.

The terrestrial inputs of dissolved inorganic nutrients (nitrate, phosphate, and silicate) were prescribed using monthly climatologies corresponding to the median value over the period 1990–2009 of the estimates provided by Ludwig et al. (2010). As terrestrial inputs influencing the carbonate system are poorly constrained and only estimates at the subregional scale are available (see e.g., Regnier et al., 2013), a major effort was put in the compilation of an observational dataset of Dissolved Inorganic Carbon and Total Alkalinity concentrations for those Mediterranean rivers with a minimum annual water discharge of 1 km³ as given in Ludwig et al. (2009). Reference concentration data for 66 rivers (see **Supplementary Table 1**) were combined with the respective annual freshwater flows to determine DIC and TA loads and missing concentrations were set equal to the average values computed over the 10 coastal sub-basins defined in Ludwig et al. (2010). Exchanges at Bosphorus Strait were set using constant values for DIC and TA as in Cossarini et al. (2015).

The coupled model components were spun up with a stepwise strategy by first running the physical component alone for



20 years and consequently using the last year to drive the biogeochemical process in a perpetual mode until the surface gas exchanges reached a stable condition, which occurred after 10 years. Afterwards, the reference experiment was performed using the time varying boundary conditions and forcing fields previously described. Alkalinization scenarios are started only 20 years within the reference experiment in order to allow for the system to return to a fully transitional, non-equilibrium state of air-sea fluxes. A brief comparison to reference data for present day conditions illustrating the feasibility of model results in the principle prognostic variables of this study is given in the **Supplementary Material** (section 3).

2.3. Alkalinization Scenarios

This regional application of ocean liming to the Mediterranean Sea explores the potential of using the existing vessel traffic as a vehicle for lime disposal. Among the variety of vessels crossing the basin, bulk carriers, and container ships were identified as the best targets to perform liming operations due to their high load capacity and the wide spatial coverage of shipping routes (Caserini et al., 2021). The traffic associated with these two ship classes, taken from monthly data of traffic density in the year 2017 available from the EMODnet-Human Activities Project (EMODnet, 2019), was translated into a monthly climatological gridded dataset of vessel time suitable for lime disposal excluding any traffic closer than 5 km to the coastline and it represents the spatial driver of the following ocean liming scenarios that are implemented over a 30 year-long time period starting from 2020. The alkalinization amounts per area and time unit are then computed from the gridded vessel time dataset by applying constant lime discharge rates of each vessel during navigation (see **Figure 1**).

Similar to previous studies (Keller et al., 2014; Lenton et al., 2018), a first scenario (CTS200) was implemented by considering a cumulative annual lime disposal of 200 Mtons over the entire basin, a technically feasible rate considering the amount of shipping traffic in the Mediterranean Sea and the typical capacity of cargo and tanker ships (Caserini et al., 2021). This rate was implemented in the model through the addition of 7.58 kg Ca(OH)₂/s to the surface TA for each ship,

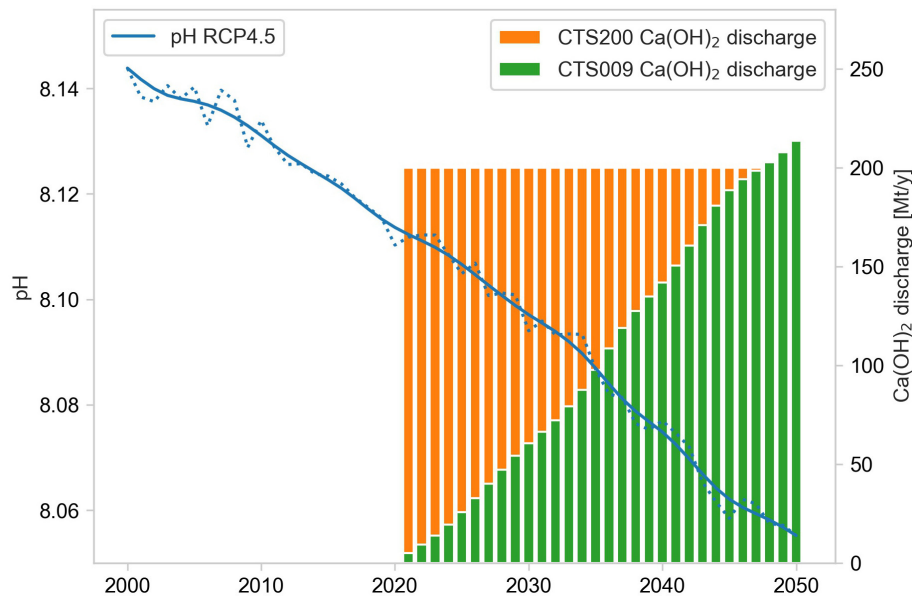


FIGURE 2 | Lime disposal over the Mediterranean basin for the CTS200 (orange) and CTS009 scenario (green) vs. mean surface pH trend of the RCP4.5 baseline scenario (blue; dotted: annual means, full line: smoothed trend).

which scaled by the time spent by vessels in a single gridpoint per month and integrated over space and time, leads to the cumulative target of 200 Mt/y and is significantly lower than the discharge of 1 tCa(OH)₂/s hypothesized in other alkalinization scenarios (e.g., Renforth et al., 2013). The sedimentation of Ca(OH)₂ has been neglected here due to its short dissolution time scales compared to its sinking velocity (Caserini et al., 2021). This scenario primarily addresses the potential of a sudden intervention to sequester atmospheric CO₂ through alkalinization and evaluates the basin wide spatial changes occurring in the carbonate system.

A more adaptive strategy, somewhat similar to the approach adopted in Ilyina et al. (2013), was applied in a second simulation (CTS009) aiming to stabilize the mean surface pH at present day values. This scenario is based on the observation that the increase of surface pH through alkalinization is at first order proportional to the lime disposal increase emerging from a series of idealized one-dimensional perturbation experiments illustrated in **Supplementary Material** (section 4). We then assumed that this linear relationship would approximately transfer to the full scale experiment if stabilization of present day pH conditions can be achieved at basin scale, an assumption ultimately to be confirmed by the result of this simulation. Hence, a time varying lime disposal was implemented with annual increments proportional to the smoothed mean surface pH trend of the baseline scenario (see **Figure 2**) leading to a cumulative discharge over the 2021–2050 period of approximately 3.2 Gt Ca(OH)₂ compared to the 6.0 Gt of the CTS200 scenario. We used the smoothed pH timeseries here in order to obtain a non-linear representation of the pH trend while maintaining the higher frequency interannual variability, which was achieved via the convolution of a Hann window function with a width of 11

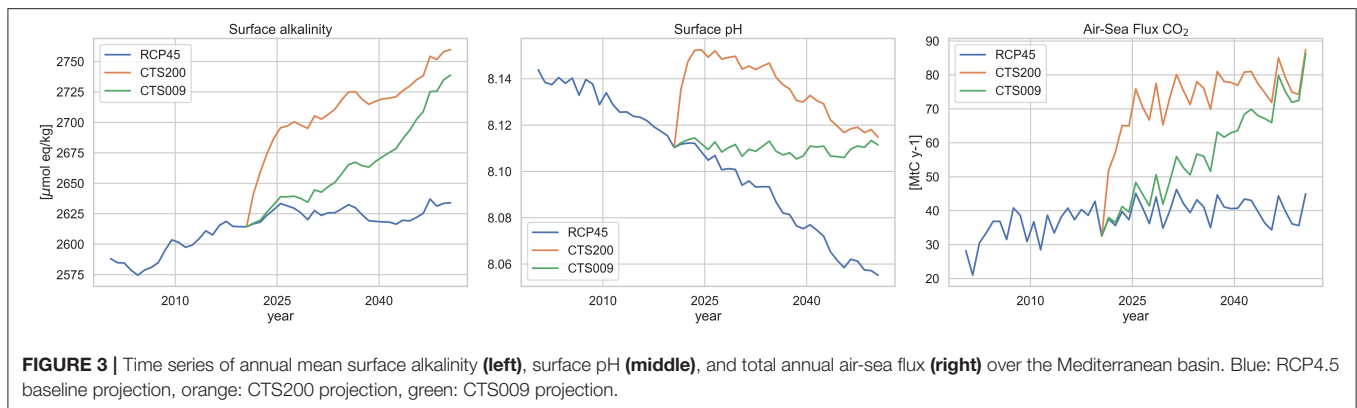
years. The conversion factor used in this scenario to compute the alkalinization levels based on the pH trend was established empirically at 0.009 pH units per (mmol Ca(OH)₂ m⁻² d⁻¹) of basin mean alkalinity addition via the adjustment of an initial guess in a brief sensitivity simulation and correcting it for the remaining pH trend.

A control simulation in perpetual mode representing the conditions of year 2000 was performed for the entire simulation period in order to identify any residual model drift ($\leq 2.5\%$), computed in the control simulation via Hann smoothing of the temporal evolution of the simulation (with the same 11 year width window used for the pH trend above) and removed from the scenario projections.

3. RESULTS

In this section we provide the results for the two alkalinization scenarios CTS200 and CTS009 investigated in this study compared to the baseline simulation RCP4.5 looking at the impact of the lime discharge on surface alkalinity and the two target indicators for the mitigation of greenhouse-gas increase and acidification, i.e., the air-sea flux of CO₂ representing the uptake of atmospheric CO₂ by the ocean and surface pH indicating the surface water acidity.

Figure 3 shows the mean surface alkalinity, pH and total air-sea flux of CO₂. The time-series for alkalinity (left) highlights a significantly different behavior for the two alkalinization strategies in terms of surface water alkalinity. Under the constant discharge scenario CTS200 (orange) it exhibits an abrupt increase in surface alkalinity by about 80 $\mu\text{mol kg}^{-1}$ over the first few years and afterwards increases much more gradually and slower



to reach about $2,760 \mu\text{mol kg}^{-1}$ by the end of the simulation, indicating significant fluxes of alkalinity from the surface to the deeper layers. For the CTS009 scenario (green) on the contrary surface alkalinity increases steadily over the entire period to reach a little lower surface average of $2,740 \mu\text{mol kg}^{-1}$ by 2050. Surface pH (center) exhibits under the constant discharge scenario CTS200 (orange) an abrupt increase of about 0.04 units over the first couple of years and afterwards resembles the trend of the baseline scenario (blue) maintaining the initial offset, while the variable discharge scenario CTS009 (green) fulfills its aim of stabilizing mean surface pH at the level of 2020 at the beginning of the alkalinization experiment. In case of the oceanic uptake of atmospheric CO_2 , the CTS200 scenario rapidly doubles the carbon sink from little less than $40 \text{ Mt CO}_2 \text{ y}^{-1}$ to almost $80 \text{ Mt CO}_2 \text{ y}^{-1}$ and subsequently largely maintains this level showing only a minimal increase over the remaining years. The CTS009 scenario gradually increases the uptake over the alkalinization period, until reaching approximately the same level as the CTS200 scenario toward the end of the experiments. The values of CO_2 of air-sea exchange and the level of surface pH obtained are coherent with estimates from previous works on the Mediterranean basin (MedSea, 2014; Palmiéri et al., 2015).

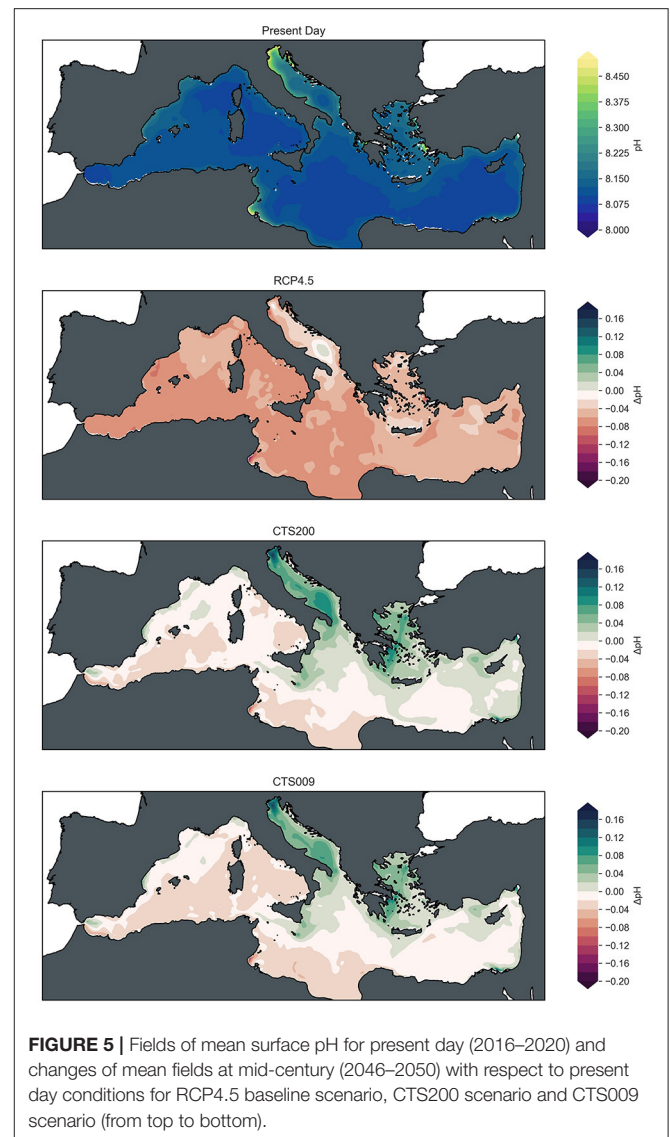
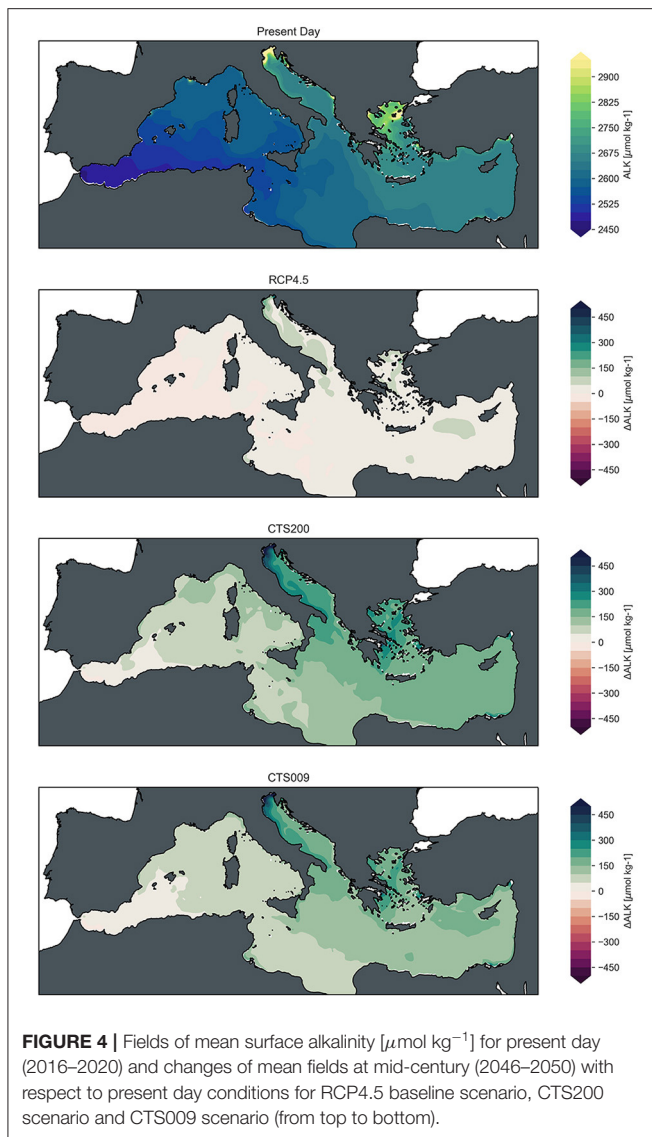
The spatial distribution of the changes induced by the alkalinization scenarios is illustrated in **Figure 4** for surface alkalinity, **Figure 5** for surface pH and **Figure 6** for air-sea flux of CO_2 . The mean present day conditions of surface alkalinity are, as to be expected, strongly correlated with surface salinity (**Supplementary Figure 1**) showing comparatively low values in the fresher waters of the Western Mediterranean along the North African coast gradually increasing toward the Levantine basin. An exception to this pattern is caused by large lateral inputs of alkalinity which lead to local extremes in surface alkalinity around the deltas of e.g., the Po and Rhone deltas and the Dardanelles. In areas of high alkalinity under present day conditions substantial increases can be observed under the RCP4.5 projected future conditions (mainly Adriatic and Aegean Sea, Northern Levantine Basin), while other areas remain comparatively stable. These changes are amplified under both alkalinization scenarios, leading to increase of alkalinity across the basin, even if at varying extent, with the exception of the Alboran Sea, the surface waters of

which are mostly of Atlantic origin where no alkalinization was applied.

Acidification of the Mediterranean under the baseline scenario RCP4.5 occurs in general across the basin with stronger acidification levels of little less than 0.1 pH units in the Western Mediterranean gradually decreasing toward the Eastern Mediterranean where acidification levels vary between 0 and 0.05 pH units. A noteworthy exception to this general pattern is presented by the Adriatic Sea with particularly low pH decreases between 0 and 0.025 pH units and increasing levels of pH in the South Adriatic Gyre. Only along the shallow North-Eastern coast slightly higher levels of acidification are reached in this sub-basin. Other areas of low acidification levels are observed in coincidence with gyres and overturning cells in the Gulf of Lions, the Cretan Sea and west of Cyprus (Robinson and Golnaraghi, 1994; Pinardi et al., 2015, **Supplementary Figure 1**).

The relative geographic pattern is largely maintained in the alkalinization scenarios, but offset toward a pH neutral basin average as shown in **Figure 3**. Under the given discharge levels, the two scenarios lead to very similar changes in surface pH conditions at mid-century with marginally higher levels for the CTS200 simulation. For both alkalinization scenarios the highest increases in pH with respect to present day conditions are reached in the Northern Adriatic and Aegean Sea with increments up to approximately 0.2 and 0.1 pH units, respectively. Various local maxima of pH can be observed coincident with the circulation features previously mentioned for the baseline changes and in the vicinity of large ports where shipping traffic and hence discharge is particularly high, e.g., nearby Valencia, Marseille, Genova, Valletta, Piraeus.

Figure 6 illustrates the general characteristics of air-sea flux pattern of CO_2 of the Mediterranean Sea acting as strong sink over large parts of the Western Mediterranean, the Adriatic, and the Aegean Sea, while the Eastern Mediterranean acts as comparatively weak sink (top-left for average present-day conditions). Most noticeable changes under RCP4.5 for mid-century (top-right) are an increased influx of CO_2 in locations corresponding to the pH changes described in the previous paragraph, i.e., in the Adriatic Sea (particularly the South Adriatic gyre with maximum increases of around $50 \text{ mg C m}^{-2} \text{ d}^{-1}$), the Aegean and Cretan Sea, the Gulf of Lions and west of Cyprus. The



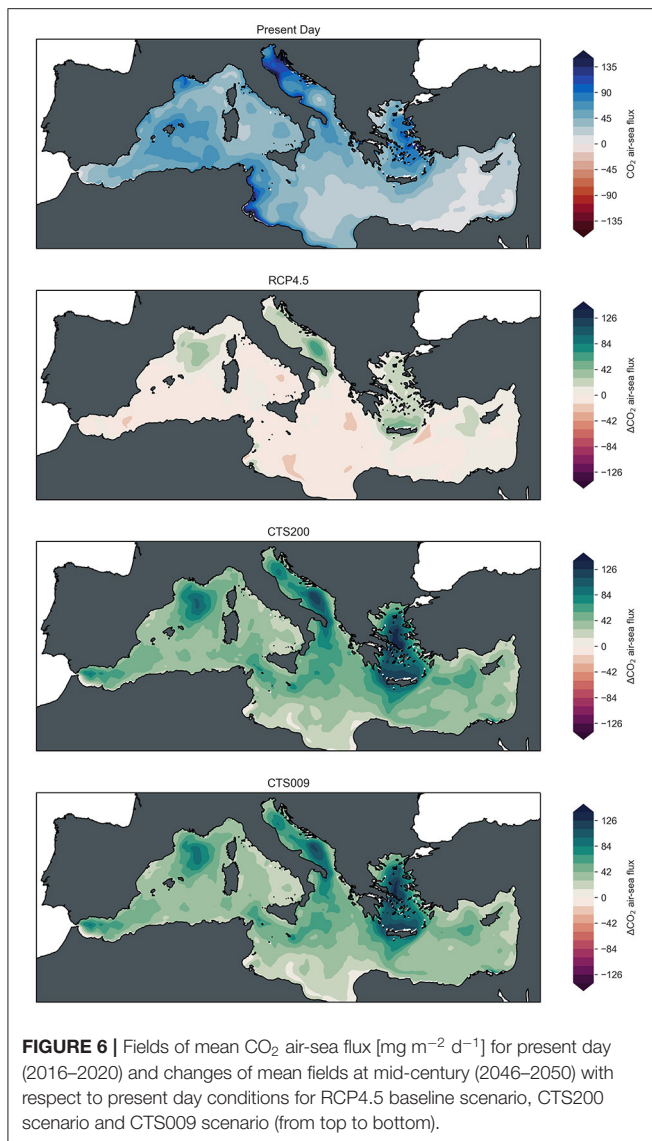
maps of changes for the two alkalinization scenarios reflect this overall pattern elevating the CO_2 uptake to positive values across the entire basin which in the South Adriatic gyre and Aegean Sea reach levels in excess of $120 \text{ mg C m}^{-2} \text{ d}^{-1}$, again with slightly stronger fluxes for the CTS200 scenario compared to the CTS009 scenario. In contrast to the pH fields, the high shipping traffic in the vicinity of ports does not seem to impact the air-sea flux pattern significantly.

Looking in more detail at these combined results some distinct features emerge in addition to these large scale patterns. In the two areas where increased shipping traffic (and therefore higher levels of alkalinization) coincides with significant lateral inputs of alkalinity and dissolved inorganic carbon and the topography of the area leads to accumulation of alkalinity, the patterns of the alkalinization scenarios diverge from those of the baseline scenario. The areas under direct influence of the lateral inputs are less sensitive to the artificial addition of alkalinity in terms of

pH and air-sea flux response, while away from the lateral inputs toward the center of the basins alkalinization induces prominent features of pH and CO_2 uptake absent in the baseline scenario. Another interesting feature are the pronounced increases of CO_2 in the future scenarios at the locations of the cyclonic gyres in the South-Adriatic and North-West Mediterranean Sea, both subject to dense water formation and convection events in winter. In these locations the increase in air-sea flux is triggered by decreased levels of DIC originating from the intermediate layer that turns these locations into efficient carbon sinks, an effect that is further accentuated in the alkalinization scenarios.

4. DISCUSSIONS

The alkalinization strategies applied in this study to the Mediterranean Sea illustrate the potential of ocean liming to mitigate climate change by increasing the air-sea flux of CO_2



across the basin and counteracting acidification. In contrast to previous studies, the analyzed scenarios offer a clear pathway into practical implementation being based on realistic levels of lime discharge using the current network of cargo and tanker shipping routes across the Mediterranean Sea as described in more detail in the accompanying work of Caserini et al. (2021). Two different approaches of alkalinization scenarios have been explored: one (CTS200) with a constant annual discharge of lime over the entire scenario period and another with gradually increasing alkalinization levels (CTS009) proportional to the pH decreases in the baseline scenario RCP4.5. It should be noted that similar to previous works on the topic this study is based on a single model projection of a single baseline scenario. Consequently, the study provides a proof of concept of the feasibility of the approaches taken, while for a full, robust quantification taking into account the various sources of uncertainty involved (e.g., scenarios, model

structure, and parametrization, internal variability) a larger set of ensemble simulations would be required.

Keeping this limitation in mind, we can state that both proposed approaches substantially increase the CO₂ sink of the Mediterranean Sea (doubling the uptake under present day conditions) and neutralize acidification in terms of the basin average pH by the end of the alkalinization period of 30 years. These conditions are achieved however on considerably different pathways. The CTS200 scenario of constant discharge provokes a rapid increase of surface pH and air-sea flux and resumes after this offset to follow the trends of the system under the baseline scenario with an annual uptake of around 70–80 MtC/y over the larger part of the simulation leading to a cumulative increase in CO₂ air-sea flux by 1.02 GtC achieved via the total discharge of 6.00 Gt Ca(OH)₂ over the full duration of the alkalinization scenario. The CTS009 scenario in contrast, gradually increases the air-sea flux toward a similar annual uptake of around 80 GtC/y at the end of the simulation, leading to a total of 0.53 GtC of air-sea flux increase discharging cumulatively 3.21 Gt Ca(OH)₂, but manages to stabilize the surface pH at present day levels. The difference between the two scenarios is particularly important with respect to the pH rise over the first couple of years in the CTS200 scenario, which exceeds twice the acidification rate occurring over a decade in the RCP4.5 scenario and hence strongly alters the alkaline environment of the Mediterranean Sea. While the ecological impacts of acidification of the ocean are subject to a wide field of research, comparatively little is known about the opposite process of alkalinization in order to appreciate the impacts of such changes on the Mediterranean Sea ecosystem. Among the side effects mentioned in literature are the potential of positive and negative feed-backs, affecting nutrient limitation of primary producers, causing physiological damage to marine organisms and altering their metabolic balance (Cripps et al., 2013; Bach et al., 2019), but more research is required on the topic in order to enable a quantified estimate of the resilience of marine ecosystems to alkalinization and an adequate risk assessment. This point is even more relevant when considering the spatial heterogeneity of alkalinization impacts illustrated in Figure 5, which shows that local extremes of pH variation may differ from the basin annual mean by more than 0.1 pH units. The location of pH maxima resulting from the map suggests the reduction of lime discharge in areas of high shipping traffic and reduced mixing with the surrounding water bodies like the Northern Adriatic and Aegean Sea. The same holds for the vicinity of large ports, where pH is strongly affected by alkalinization in contrast to areas of dense traffic but effective redistribution via ocean currents, e.g., Gibraltar and Alboran Sea in order to avoid damaging effects to the local ecosystems. Similarly, the results for the Aegean and Adriatic Sea suggest, that it might be beneficial to reduce alkalinization in areas where other large sources of alkalinity seem to reduce the efficiency of the process. In contrast, while generally the increase of stratification across the basin reduces the carbon sink of the Mediterranean Sea, its cyclonic gyres that are associated with dense water formation appear increasingly efficient in absorbing atmospheric carbon, suggesting that increased alkalinization in areas feeding into these gyres may be beneficial. Nevertheless, the present study does

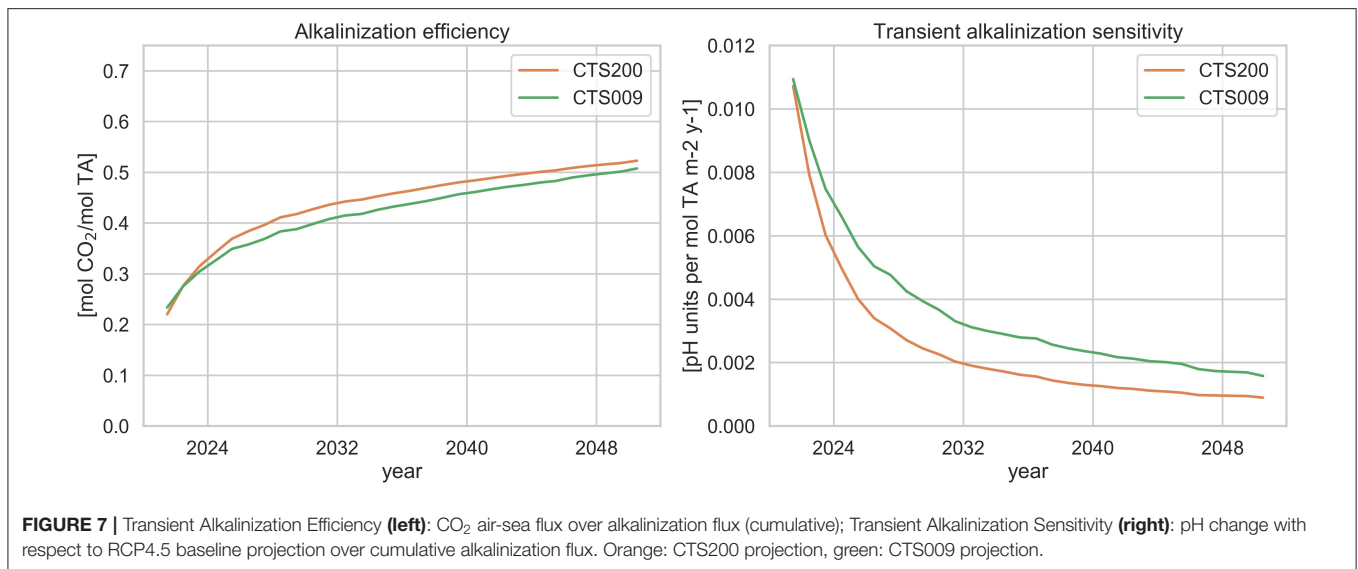


FIGURE 7 | Transient Alkalinization Efficiency (**left**): CO₂ air-sea flux over alkalization flux (cumulative); Transient Alkalinization Sensitivity (**right**): pH change with respect to RCP4.5 baseline projection over cumulative alkalization flux. Orange: CTS200 projection, green: CTS009 projection.

provide only a first indication toward the role of these features and their interaction with alkalization strategies, more detailed and targeted studies are required for a more conclusive picture.

In order to fully appreciate the different potential of the two alkalization pathways and given that the two scenarios apply different total amounts of lime and distribution of discharge over the alkalization period even though reaching similar levels of air-sea flux and pH by the end of the scenarios, we put into relation lime discharge, air-sea flux and the pH changes with respect to the RCP4.5 baseline scenario. To this purpose we define two indicators: the transient alkalization efficiency as the ratio of cumulative CO₂ air-sea flux increase over the cumulative added alkalinity and the transient alkalization sensitivity as the ratio of change of mean surface pH with respect to the no alkalization case over the cumulative added alkalinity.

Figure 7 shows the temporal evolution of these two indicators in the Mediterranean Sea over the alkalization period for both liming scenarios. The transient alkalization efficiency (left), which describes the CO₂ uptake potential of the alkalization approach, starts at a value of little more than 0.2 mol CO₂ (mol TA)⁻¹ and reaches up to 0.5 mol CO₂ (mol TA)⁻¹ with slightly higher values (by about 3%) for the constant discharge scenario. These values are substantially lower than the upper bound of 1 mol CO₂ (mol TA)⁻¹ given by the consumption of aqueous CO₂ in Equation (1), due to two processes: the redistribution of inorganic dissolved carbon species toward a new equilibrium of the carbonate system and dynamic exchanges with the underlying water bodies further reducing the efficiency. They are also lower than the estimate of 0.8 mol CO₂ (mol TA)⁻¹ in Renforth et al. (2013), who however did not involve the latter process and the estimate of 0.7 mol CO₂ (mol TA)⁻¹ in Keller et al. (2014), but are consistent with the efficiency estimates given recently by Köhler (2020) for the near future in a multimillennial alkalization experiment.

The transient alkalization sensitivity (right), which describes the mean pH response of the system under alkalization

relative to the added alkalinity, is maximal at the beginning of the alkalization period at about 0.11 pH units per mol TA m⁻² y⁻¹ and gradually decreasing to values of approximately 0.0016 and 0.0009 for the scenarios CTS009 and CTS2000, respectively. Hence, over the full alkalization period, the gradually increasing approach reveals a substantially higher potential in counteracting ocean acidification than the constant discharge scenario whose cumulative sensitivity at the end of the period is about 44% lower. Note, that the sensitivities after the first year of the simulations CTS200 and CTS009 are nearly identical confirming that the sensitivity is independent of the alkalization levels as long as the environmental conditions are not altered significantly, confirming the observation emerging from the idealized 1D experiments.

The substantially higher potential in counteracting acidification along with the avoidance of the abrupt changes in surface pH suggests that the approach of gradually increasing discharge following the acidification trend of the system without alkalization is favorable in ecological and economic terms over the application of constant discharge rates, even if the latter appears slightly more efficient in terms of CO₂ uptake. It should be noted here that an actual implementation of any of these approaches should be preceded by a complete analysis of all costs and benefits taking into consideration the full chain of processes involved, including the production and transport of lime.

In conclusion, this study illustrates how technically feasible amounts of alkalization allow to counteract the threat of ocean acidification and to remove CO₂ from the atmosphere, through a substantial increase in CO₂ uptake across the Mediterranean Sea. The preferred approach consists of gradually increasing lime discharge levels using the existing network of cargo and tanker ships, stabilizing the mean surface pH at present day values using the existing network of cargo and tanker ships. Ecological impacts and side-effects, particularly in local areas of high alkalization levels due to denser ship

traffic and accumulation via ocean dynamics remain to be carefully assessed.

DATA AVAILABILITY STATEMENT

The datasets analyzed in this study can be found in the Zenodo repository (doi: 10.5281/zenodo.4068027). Additional data is available from the corresponding author on request.

AUTHOR CONTRIBUTIONS

MB developed the design of this study, performed the model simulations, and wrote the manuscript. TL assisted in the design of the study, in the preparation of the simulations, and in the writing of the manuscript and the supplements. SM, SC, and

MG assisted in the design of the study and the writing of the manuscript. All authors contributed to the article and approved the submitted version.

FUNDING

The research was carried out within the Desarc-Maresanus project (www.desarc-maresanus.net), which received the financial support of Amundi SGR SpA.

SUPPLEMENTARY MATERIAL

The Supplementary Material for this article can be found online at: <https://www.frontiersin.org/articles/10.3389/fclim.2021.614537/full#supplementary-material>

REFERENCES

- Bach, L. T., Gill, S. J., Rickaby, R. E. M., Gore, S., and Renforth, P. (2019). CO₂ removal with enhanced weathering and ocean alkalinity enhancement: potential risks and co-benefits for marine pelagic ecosystems. *Front. Clim.* 1:7. doi: 10.3389/fclim.2019.00007
- Caserini, S., Barreto, B., Lanfredi, C., Cappello, G., Ross Morrey, D., and Grosso, M. (2019). Affordable CO₂ negative emission through hydrogen from biomass, ocean liming, and CO₂ storage. *Mitigat. Adapt. Strat. Glob. Change* 24, 1231–1248. doi: 10.1007/s11027-018-9835-7
- Caserini, S., Pagano, D., Campo, F., Abbá, A., De Marco, S., Righi, D., et al. (2021). Potential of maritime transport for ocean liming and atmospheric CO₂ removal. *Front. Clim.* 3. doi: 10.3389/fclim.2021.575900
- Cossarini, G., Lazzari, P., and Solidoro, C. (2015). Spatiotemporal variability of alkalinity in the mediterranean sea. *Biogeosciences* 12, 1647–1658. doi: 10.5194/bg-12-1647-2015
- Cripps, G., Widdicombe, S., Spicer, J. I., and Findlay, H. S. (2013). Biological impacts of enhanced alkalinity in *carcinus maenas*. *Mar. Pollut. Bull.* 71, 190–198. doi: 10.1016/j.marpolbul.2013.03.015
- Data-Driven EnviroLab and NewClimate Institute (2020). *Accelerating Net Zero: Exploring Cities, Regions, and Companies' Pledges to Decarbonise*. Technical report, NewClimate Institute. Available online at: https://newclimate.org/wp-content/uploads/2020/09/NewClimate_Accelerating_Net_Zero_Sept2020.pdf
- EMODnet (2019). *Shipping Density*. Available online at: <https://www.emodnet-humanactivities.eu/view-data.php>
- Friedlingstein, P., Jones, M. W., O'Sullivan, M., Andrew, R. M., Hauck, J., Peters, G. P., et al. (2019). Global carbon budget 2019. *Earth Syst. Sci. Data* 11, 1783–1838. doi: 10.5194/essd-11-1783-2019
- Gattuso, J.-P., Magnan, A., Billé, R., Cheung, W. W. L., Howes, E. L., Joos, F., et al. (2015). Contrasting futures for ocean and society from different anthropogenic CO₂ emissions scenarios. *Science* 349:aac4722. doi: 10.1126/science.aac4722
- Giorgi, F. (2006). Climate change hot-spots. *Geophys. Res. Lett.* 33, 1–4. doi: 10.1029/2006GL025734
- González, M. F., and Ilyina, T. (2016). Impacts of artificial ocean alkalinization on the carbon cycle and climate in earth system simulations. *Geophys. Res. Lett.* 43, 6493–6502. doi: 10.1002/2016GL068576
- Hoegh-Guldberg, O., Jacob, D., Taylor, M., Bindi, M., Brown, S., Camilloni, I., et al. (2018). "Impacts of 1.5°C global warming on natural and human systems," in *Global Warming of 1.5°C. An IPCC Special Report on the Impacts of Global Warming of 1.5°C Above Pre-Industrial Levels and Related Global Greenhouse Gas Emission Pathways, in the Context of Strengthening the Global Response to the Threat of Climate Change, Sustainable Development, and Efforts to Eradicate Poverty*. Intergovernmental Panel on Climate Change. Available online at: <https://www.ipcc.ch/sr15/chapter/chapter-3/>
- Ilyina, T., Wolf-Gladrow, D., Munhoven, G., and Heinze, C. (2013). Assessing the potential of calcium-based artificial ocean alkalinization to mitigate rising atmospheric CO₂ and ocean acidification. *Geophys. Res. Lett.* 40, 5909–5914. doi: 10.1002/2013GL057981
- IPCC (2013). *Climate Change 2013: The Physical Science Basis. Contribution of Working Group I to the Fifth Assessment Report of the Intergovernmental Panel on Climate Change*. Cambridge University Press.
- IPCC (2018). "Summary for policymakers," in *Global Warming of 1.5°C. An IPCC Special Report on the Impacts of Global Warming of 1.5°C Above Pre-Industrial Levels and Related Global Greenhouse Gas Emission Pathways, in the Context of Strengthening the Global Response to the Threat of Climate Change, Sustainable Development, and Efforts to Eradicate Poverty*, eds V. Masson-Delmotte, P. Zhai, H.-O. Pörtner, D. Roberts, J. Skea, P. Shukla, A. Pirani, W. Moufouma-Okia, C. Péan, R. Pidcock, S. Connors, J. Matthews, Y. Chen, X. Zhou, M. Gomis, E. Lonnoy, T. Maycock, M. Tignor, and T. Waterfield (World Meteorological Organization), 32. Available online at: <https://www.ipcc.ch/sr15/chapter/spm/>
- IPCC (2019). "Summary for policymakers," in *IPCC Special Report on the Ocean and Cryosphere in a Changing Climate*, eds H. O. Pörtner, D. Roberts, V. Masson-Delmotte, M. T. Zhai, E. Poloczanska, K. Mintenbeck, A. Alegría, M. Nicolai, A. Okem, J. Petzold, B. Rama, and N. Weyer. Available online at: <https://www.ipcc.ch/srocc/chapter/summary-for-policymakers/>
- Keller, D. P., Feng, E. Y., and Oschlies, A. (2014). Potential climate engineering effectiveness and side effects during a high carbon dioxide-emission scenario. *Nat. Commun.* 5, 1–11. doi: 10.1038/ncomms4304
- Khatiwala, S., Tanhua, T., Mikaloff Fletcher, S., Gerber, M., Doney, S. C., Graven, H. D., et al. (2013). Global ocean storage of anthropogenic carbon. *Biogeosciences* 10, 2169–2191. doi: 10.5194/bg-10-2169-2013
- Köhler, P. (2020). Anthropogenic CO₂ of high emission scenario compensated after 3500 years of ocean alkalinization with an annually constant dissolution of 5 Pg of olivine. *Front. Clim.* 2:575744. doi: 10.3389/fclim.2020.575744
- Kroeker, K. J., Kordas, R. L., Crim, R., Hendriks, I. E., Ramajo, L., Singh, G. S., et al. (2013). Impacts of ocean acidification on marine organisms: quantifying sensitivities and interaction with warming. *Glob. Change Biol.* 19, 1884–1896. doi: 10.1111/gcb.12179
- Lacoue-Labarthe, T., Nunes, P. A., Ziveri, P., Cinar, M., Gazeau, F., Hall-Spencer, J. M., et al. (2016). Impacts of ocean acidification in a warming Mediterranean Sea: an overview. *Region. Stud. Mar. Sci.* 5, 1–11. doi: 10.1016/j.rsmas.2015.12.005
- Lazzari, P., Solidoro, C., Ibello, V., Salon, S., Teruzzi, A., Béranger, K., et al. (2012). Seasonal and inter-annual variability of plankton chlorophyll and primary production in the Mediterranean Sea: a modelling approach. *Biogeosciences* 9, 217–233. doi: 10.5194/bg-9-217-2012

- Lenton, A., Matear, R. J., Keller, D. P., Scott, V., and Vaughan, N. E. (2018). Assessing carbon dioxide removal through global and regional ocean alkalinization under high and low emission pathways. *Earth Syst. Dyn.* 9, 339–357. doi: 10.5194/esd-9-339-2018
- Lovato, T., and Vichi, M. (2015). An objective reconstruction of the Mediterranean sea carbonate system. *Deep Sea Res. Part I Oceanogr. Res. Pap.* 98, 21–30. doi: 10.1016/j.dsr.2014.11.018
- Lovato, T., Vichi, M., and Oddo, P. (2013). *High-Resolution Simulations of Mediterranean Sea Physical Oceanography Under Current and Scenario Climate Conditions: Model Description, Assessment and Scenario Analysis*. CMCC Research Paper. Available online at: <https://www.cmcc.it/wp-content/uploads/2014/02/rp0207-ans-12-2013.pdf>
- Ludwig, W., Bouwman, A., Dumont, E., and Lespinas, F. (2010). Water and nutrient fluxes from major mediterranean and black sea rivers: past and future trends and their implications for the basin-scale budgets. *Glob. Biogeochem. Cycles* 24, 1–14. doi: 10.1029/2009GB003594
- Ludwig, W., Dumont, E., Meybeck, M., and Heussner, S. (2009). River discharges of water and nutrients to the Mediterranean and Black Sea: major drivers for ecosystem changes during past and future decades? *Prog. Oceanogr.* 80, 199–217. doi: 10.1016/j.pocean.2009.02.001
- Madec, G., Benschila, R., Bricaud, C., Coward, A., Dobricic, S., Furner, R., et al. (2013). *NEMO Ocean Engine. Note du Pole de Modélisation 27*, Institut Pierre-Simon Laplace (IPSL), France.
- MedSea (2014). *Final Project Report*. Technical report, Mediterranean Sea Acidification in a changing climate, EU FP7 265103. Available online at: <https://cordis.europa.eu/docs/results/265/265103/final1-project-final-report-lastdraft-3.pdf>
- Millot, C., and Taupier-Letage, I. (2005). “Circulation in the Mediterranean sea,” in *The Mediterranean Sea, Handbook of Environmental Chemistry*, ed A. Saliot (Springer), 29–66. doi: 10.1007/b107143
- Moss, R. H., Edmonds, J. A., Hibbard, K. A., Manning, M. R., Rose, S. K., Van Vuuren, D. P., et al. (2010). The next generation of scenarios for climate change research and assessment. *Nature* 463, 747–756. doi: 10.1038/nature08823
- Oddo, P., Adani, M., Pinardi, N., Fratianni, C., Tonani, M., Pettenuzzo, D., et al. (2009). A nested Atlantic-Mediterranean Sea general circulation model for operational forecasting. *Ocean Sci.* 5, 461–473. doi: 10.5194/os-5-461-2009
- Olsen, A., Key, R. M., Van Heuven, S., Lauvset, S. K., Velo, A., Lin, X., et al. (2016). The global ocean data analysis project version 2 (GLODAPv2)—an internally consistent data product for the world ocean. *Earth Syst. Sci. Data* 8, 297–323. doi: 10.5194/essd-8-297-2016
- Orr, J. C., Najjar, R. G., Aumont, O., Bopp, L., Bullister, J. L., Danabasoglu, G., et al. (2017). Biogeochemical protocols and diagnostics for the CMIP6 Ocean Model Intercomparison Project (OMIP). *Geosci. Model Dev.* 10, 2169–2199. doi: 10.5194/gmd-10-2169-2017
- Palmiéri, J., Orr, J. C., Dutay, J.-C., Béranger, K., Schneider, A., Beuvier, J., et al. (2015). Simulated anthropogenic CO₂ storage and acidification of the Mediterranean Sea. *Biogeosciences* 12, 781–802. doi: 10.5194/bg-12-781-2015
- Pinardi, N., Cessi, P., Borile, F., and Wolfe, C. L. P. (2019). The Mediterranean Sea overturning circulation. *J. Phys. Oceanogr.* 49, 1699–1721. doi: 10.1175/JPO-D-18-0254.1
- Pinardi, N., Zavatarelli, M., Adani, M., Coppini, G., Fratianni, C., Oddo, P., et al. (2015). Mediterranean Sea large-scale low-frequency ocean variability and water mass formation rates from 1987 to 2007: a retrospective analysis. *Prog. Oceanogr.* 132, 318–332. doi: 10.1016/j.pocean.2013.11.003
- Regnier, P., Friedlingstein, P., Ciais, P., Mackenzie, F. T., Gruber, N., Janssens, I. A., et al. (2013). Anthropogenic perturbation of the carbon fluxes from land to ocean. *Nat. Geosci.* 6, 597–607. doi: 10.1038/ngeo1830
- Renforth, P., Jenkins, B. G., and Kruger, T. (2013). Engineering challenges of ocean liming. *Energy* 60, 442–452. doi: 10.1016/j.energy.2013.08.006
- Renforth, P., and Wilcox, J. (2020). Editorial: The role of negative emission technologies in addressing our climate goals. *Front. Clim.* 2:1. doi: 10.3389/fclim.2020.00001
- Robinson, A. R., and Golnaraghi, M. (1994). *The Physical and Dynamical Oceanography of the Mediterranean Sea*. NATO ASI Series. Dordrecht: Springer Netherlands, 255–306. doi: 10.1007/978-94-011-0870-6_12
- Schellnhuber, H. J., Rahmstorf, S., and Winkelmann, R. (2016). Why the right climate target was agreed in Paris. *Nat. Clim. Change* 6, 649–653. doi: 10.1038/nclimate3013
- Scoccimarro, E., Gualdi, S., Bellucci, A., Sanna, A., Giuseppe Fogli, P., Manzini, E., et al. (2011). Effects of tropical cyclones on ocean heat transport in a high-resolution coupled general circulation model. *J. Clim.* 24, 4368–4384. doi: 10.1175/2011JCLI4104.1
- Soto-Navarro, J., Jordá, G., Amores, A., Cabos, W., Somot, S., Sevault, F., et al. (2020). Evolution of Mediterranean Sea water properties under climate change scenarios in the Med-CORDEX ensemble. *Clim. Dyn.* 54, 2135–2165. doi: 10.1007/s00382-019-05105-4
- Tokarska, K. B., Stolpe, M. B., Sippel, S., Fischer, E. M., Smith, C. J., Lehner, F., et al. (2020). Past warming trend constrains future warming in CMIP6 models. *Sci. Adv.* 6:eaz9549. doi: 10.1126/sciadv.aaz9549
- UNEP/MAP (2017). *Mediterranean Quality Status Report*. Technical report, United Nations Environment/Mediterranean Action Plan Barcelona Convention Secretariat. Available online at: <https://www.medqsr.org/>
- UNFCCC (2020). *NDC Registry*. Available online at: <https://www4.unfccc.int/sites/NDCStaging/Pages/LatestSubmissions.aspx> (accessed September 30, 2020).
- Vichi, M., Lovato, T., Butenschön, M., Tedesco, L., Lazzari, P., Cossarini, G., et al. (2020). *The Biogeochemical Flux Model (BFM): Equation Description and User Manual. BFM Version 5.2*. BFM Report Series 1, BFM Consortium. Bologna. Available online at: https://cmcc-foundation.github.io/www/bfm-community.eu/files/bfm-V5.2.0-manual_r1.2_202006.pdf
- Vichi, M., Navarra, A., and Fogli, P. (2013). Adjustment of the natural ocean carbon cycle to negative emission rates. *Clim. Change* 118, 105–118. doi: 10.1007/s10584-012-0677-0
- Visinelli, L., Masina, S., Vichi, M., Storto, A., and Lovato, T. (2016). Impacts of data assimilation on the global ocean carbonate system. *J. Mar. Syst.* 158, 106–119. doi: 10.1016/j.jmarsys.2016.02.011
- von Schuckmann, K., Cheng, L., Palmer, M. D., Hansen, J., Tassone, C., Aich, V., et al. (2020). Heat stored in the earth system: where does the energy go? *Earth Syst. Sci. Data* 12, 2013–2041. doi: 10.5194/essd-12-2013-2020
- Williamson, P. (2016). Emissions reduction: scrutinize CO₂ removal methods. *Nat. News* 530:153. doi: 10.1038/530153a
- Zeebe, R. W., and Wolf-Gladrow, D. (2001). *CO₂ in Seawater: Equilibrium, Kinetics, Isotopes*. Elsevier Oceanography Series. Elsevier. Available online at: <https://www.elsevier.com/books/co2-in-seawater-equilibrium-kinetics-isotopes/zeebe/978-0-444-50946-8>

Conflict of Interest: The authors declare that the research was conducted in the absence of any commercial or financial relationships that could be construed as a potential conflict of interest.

Copyright © 2021 Butenschön, Lovato, Masina, Caserini and Grosso. This is an open-access article distributed under the terms of the Creative Commons Attribution License (CC BY). The use, distribution or reproduction in other forums is permitted, provided the original author(s) and the copyright owner(s) are credited and that the original publication in this journal is cited, in accordance with accepted academic practice. No use, distribution or reproduction is permitted which does not comply with these terms.